PHYSICAL REVIEW B VOLUME 51, NUMBER 1 1 JANUARY 1995-I

Mössbauer characterization of γ-FeSi$_2$ precipitates in Si(100)

J. Desimoni, F. H. Sánchez, and M. B. Fernández van Raap
Departamento de Física, Facultad de Ciencias Exactas, Universidad Nacional de La Plata, Casilla de Correo No. 67, (1900) La Plata, Argentina

H. Bernas and C. Clerc
Centre de Spectrométrie Nucléaire et Spectrométrie de Masse, 91405 Orsay Campus, France

X. W. Lin
Materials Science Division, Lawrence Berkeley Laboratory, Berkeley, California 94720

(Received 10 June 1994)

Metastable γ-FeSi$_2$ fluorite-type was formed as precipitates in Si(100) by room-temperature ^{57}Fe implantation, followed by ion-beam-induced epitaxial crystallization at 593 K. In spite of the cubic structure of γ-FeSi$_2$, the Mössbauer spectrum consists of two broad lines, rather than a single line. It is best described by means of a smooth distribution of electric field gradients with nearly the same isomer shift ($\delta_{\mathrm{IS}}=0.198$ mm/s) for each gradient. After thermal treatments at 773 K the distribution narrows and a finite probability occurrence frequency for zero gradient appears. As the structure of ideal γ-FeSi$_2$ consists of Si cubes alternately filled with Fe atoms, it is suggested that the distribution arises from misplacement of Fe atoms to empty Si cubes in the lattice. The dependence with thermal treatments and the evolution towards β-FeSi$_2$ are discussed.

INTRODUCTION

In recent years, effort has been devoted to the study of transition-metal silicides due to their potential applications in micro- and optoelectronics.[1,2] Recently, molecular beam epitaxy (MBE) (Refs. 3 and 4) and solid phase epitaxy[5] experiments were performed to obtain epitaxial layers of iron silicides on Si. During the course of those experiments, new metastable iron silicide phases were discovered. These phases are γ-FeSi$_2$ and pseudomorphic FeSi$_{1+x}$ ($0 \leq x \leq 1$). The fluorite-type γ-FeSi$_2$ phase is metallic and probably magnetic,[6] and the pseudomorphic phase, grown on Si(111) by MBE at room temperature, has been described as a CsCl-derived defect phase with a statistical occupation of metal sites.[3] Hall resistivity measurements[7] at helium temperature, of a 33 nm thick γ-FeSi$_2$ film showed a rapid linear resistivity rise with increasing field followed by a second linear portion having a smaller slope. This behavior was interpreted as coming from two additive contributions, the first being the normal Hall effect and the second the strongly temperature-dependent anomalous Hall effect characteristic of magnetic materials.

γ-FeSi$_2$ was also obtained in the form of precipitates in Si(100) using low-dose Fe implantation and subsequent ion-beam-induced epitaxial crystallization (IBIEC).[8] This preparation technique is very reliable. It is known that for implantation with doses corresponding to Fe concentrations lower than 7 at. %, followed by IBIEC with Si beam at temperatures below 593 K, the crystal structure of the precipitates is always fluorite-type.

Structural characterization of these phases has been mainly performed by high-resolution transmission electron microscopy (TEM), reflection high-energy electron diffraction, and ion channeling techniques. Mössbauer spectroscopy (MS) is a well-suited technique to investigate the atomic and electronic surroundings of the atom probe (^{57}Fe). Although MS has been extensively used for the characterization of the stable phases α-FeSi$_2$, β-FeSi$_2$, Fe$_3$Si, and FeSi,[9,10] little work has been done on epitaxially grown metastable phases.[11]

In this paper we present Mössbauer characterization of γ-FeSi$_2$ precipitates embedded in Si(100) produced by low-dose ^{57}Fe implantation followed by IBIEC at 593 K. Subsequent thermal annealing was carried out to investigate the thermal evolution of the hyperfine parameters. Looking for magnetic interactions, MS data were recorded at 17 K. Rutherford backscattering spectroscopy (RBS) and TEM were used to complete the sample characterization.

EXPERIMENT

150 keV ^{57}Fe$^+$ ions were implanted into Si(100) at room temperature up to a dose of 2×10^{16} ions/cm^2 (atomic peak concentration $C_p=4$ at. %) at the Centre de Spectrométrie Nucléaire et Spectrométrie de Masse.[12] An amorphous region around 300 nm thick, with Fe dissolved in a buried region about 80 nm thick, was created. After implantation, a 500 keV Si beam was used to induce epitaxial crystallization of the sample, while keeping the sample holder at 593 K.

Conversion electron Mössbauer spectroscopy (CEMS) experiments were carried out in a conventional constant acceleration spectrometer at the Departamento de Física, Facultad de Ciencias Exactas, Universidad Nacional de

La Plata. A 10 mCi ^{57}CoRh source was used to obtain the 14.4 keV γ rays of ^{57}Fe. The conversion and Auger electrons coming from the resonant decay of ^{57}Fe nuclei in the absorber sample were detected with a He 94%-methane gas admixture flux detector in which samples were electrically attached to the cathode. For the data analysis two types of nonlinear least-squares fits were performed: a continuous distribution of quadrupole splittings (Δ_{QS}) allowing a linear correlation with the isomer shift (δ_{IS}) using a routine provided by Vandenberghe[13] and a routine allowing simultaneous presence of several independent quadrupole interactions. Both routines used Lorentzian functions for the component subspectra. For spectra taken after IBIEC and after thermal treatments at 733 K both fitting procedures led to mutually consistent results. However, the first method was preferred, in view of the smoothness of the Δ_{QS} distribution (see Fig. 2). Conversely, for the spectra obtained after annealing at higher temperatures, the second method was used since the development of clear differentiated probe sites was apparent.

The sample structure was characterized by cross-sectional TEM at the Materials Science Division, Lawrence Berkeley Laboratory. TEM specimens with Si[110] normal to the surface were prepared by mechanical polishing and ion milling.

Thermal treatments were done in a conventional electric oven with samples encapsulated in glass tubes under vacuum better than 8×10^{-6} Torr. Low-temperature Mössbauer measurements were carried out using a cyrogenic system in transmission geometry.

RESULTS

Only the presence of γ-FeSi$_2$ in our IBIEC-treated samples was observed by TEM, in agreement with previous experiments.[8] The γ-FeSi$_2$ phase was found to be stable at 733 K for annealings up to 2 h. TEM results of a sample annealed for 1 h are presented in Fig. 1. It can be seen that γ-FeSi$_2$ precipitates are distributed in a region about 90 nm wide and centered around 90 nm deep below the surface [Fig. 1(a)]. Both *A*- and *B*-type γ-FeSi$_2$ precipitates ≈ 5 nm in diameter can be recognized by high-resolution TEM [Fig. 2(b)]. Electron diffraction [Fig. 1(c)] confirms the cubic structure (i.e., the γ phase) of precipitates. This is because the diffraction spots, together with double diffraction from the FeSi$_2$ precipitates, divide the $g=\mathrm{Si}\langle 111\rangle$ vectors into three equal parts in reciprocal space, suggesting that FeSi$_2$ is cubic with a lattice parameter nearly identical to that of Si matrix.[14] Note that a residual amorphous surface layer ≈ 3 nm thick can be noticed in Fig. 1(a) due to incomplete IBIEC.

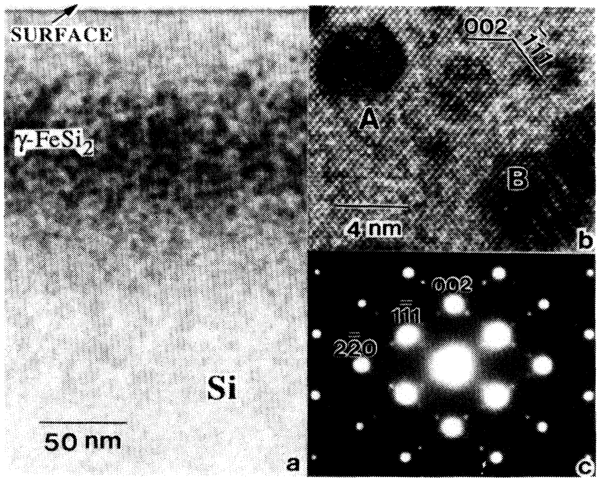

FIG. 1. TEM micrographs showing the presence of γ-FeSi$_2$ precipitates in an Fe-implanted Si sample first treated by IBIEC at 593 K and subsequently annealed at 773 K for 1 h. (a) Cross-sectional bright-field image showing the distribution of γ-FeSi$_2$ precipitates (dark region below the surface). (b) High-resolution image of *A*-type and *B*-type γ-FeSi$_2$ precipitates, viewed along Si[110]. (c) Selected-area diffraction spots correspond to reflections from the Si[110] zone axis, while the weak ones are due to reflections from *B*-type γ-FeSi$_2$ precipitates, combined with double diffraction effects.

In view of the cubic structure of γ-FeSi$_2$, a single line is expected for the Mössbauer spectrum. However, the spectrum shown in Fig. 2(a) (after IBIEC) consists of a broad symmetric doublet centered at a positive velocity. The best fit corresponds to a broad Δ_{QS} distribution (full width at half maximum $\sigma_{QS}=0.523$ mm/s) with maximum occurrence frequency at $\Delta_{QS}^{max}=0.570$ mm/s, average value $\Delta_{QS}^{av}=0.581$ mm/s [Fig. 2(b)], and $\delta_{IS}=0.198$ mm/s for all subspectra. The hyperfine parameters are shown in Table I. After thermal annealing at 733 K for 30 min, changes were observed in the CEMS spectrum [Figs. 2(c) and 2(e)]: the valley becomes shallower and the Δ_{QS} distribution becomes slightly asymmetric as a

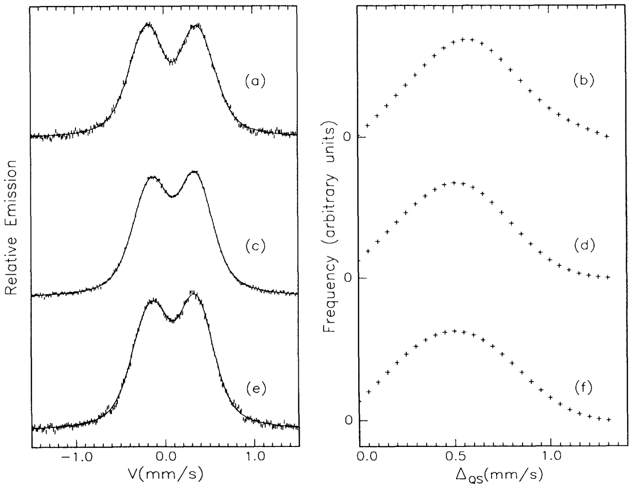

FIG. 2. (Left) γ-FeSi$_2$ room-temperature (RT) CEMS spectra. From top to bottom: after RT Fe$^+$ implantation plus 593 K Si-beam induced epitaxial crystallization, annealed 30 min at 773 K, and 60 min at the same temperature. (Right) Δ_{QS} distributions corresponding to spectra on the left.

TABLE I. Fitted hyperfine parameters after IBIEC and after thermal annealing at 773 K during a time (t), δ_{IS}, the isomer shift Δ_{QS}^{max} the more probable quadrupole splitting, Δ_{QS}^{av} the average of quadrupole splittings, σ_{QS} the full width at half maximum of the Δ_{QS} distribution, and $P(0)$ the frequency of occurrence of null EFG.

T (K)	t (min)	δ_{IS} (mm/s)	Δ_{QS}^{max} (mm/s)	Δ_{QS}^{av} (mm/s)	σ_{QS} (mm/s)	$P(0)$
		0.198	0.570	0.581	0.523	0.00
733	30	0.206	0.525	0.511	0.445	1.34
733	60	0.208	0.500	0.504	0.447	1.66
733	120	0.208	0.500	0.497	0.425	1.78

consequence of the development of a narrow isomer shift distribution centered at 0.206 mm/s. Contribution at $\Delta_{QS}=0.00$ mm/s appears with a finite frequency $P(0)=1.34$ [Fig. 3(a)]. In addition, the distribution becomes narrower and the maximum Δ_{QS}^{max} corresponds to $\Delta_{QS}=0.525$ mm/s [see Fig. 3(c)], while the associated δ_{IS} increases [Fig. 3(b)]. These results indicate that the symmetry of the charge distribution around Fe atoms increases. It should be mentioned that this thermal treatment was observed to reduce the minimum yield of RBS/channeling backscattered ions and was considered to improve ordering of the Si/γ-FeSi$_2$ system prepared by IBIEC.[8] Subsequent annealing at the same temperature (up to a total of 2 h) did not produce important changes in the hyperfine parameters, but $P(0)=1.78$ increases. Measurements performed at 17 K showed no sign of magnetic ordering.

After annealing at 923 K for 30 min, the quadrupole interaction appears different. The shape of the spectrum indicates the existence of clearly distinctive probe sites instead of the previous smooth distribution of iron environments. However, the hyperfine parameters of the interactions which sum up to the theoretical spectrum (fit) cannot be readily assigned to known silicide phases. Further thermal annealing at 1073 and 1173 K induced the transformation towards β-FeSi$_2$. The final spectrum (see Fig. 4) became narrower. It can be characterized by the two hyperfine interactions associated with β-FeSi$_2$ ($\Delta_{QS}=0.400$ mm/s, $\delta_{IS}=0.130$ mm/s and $\Delta_{QS}=0.420$ mm/s, $\delta_{IS}=0.010$ mm/s) (Refs. 9 and 10) equally populated.

DISCUSSION AND CONCLUSION

TEM experiments performed on the recrystallized samples indicate that only γ-FeSi$_2$ precipitates are formed in the Si(100) matrix. In spite of the fluorite-type structure of γ-FeSi$_2$, the MS spectra show a broad quadrupole splitting distribution in place of an expected single line. The fitted hyperfine interactions cannot be ascribed either to the known Fe-Si stable compounds[9,10] or to substitutional or interstitial iron atoms in the Si matrix.[15] Channeling experiments indicated that the minimum relative yield χ_m from iron is about 60% while it is around 14% from Si. After thermal annealing at 733 K, χ_m changes to 55 and 15 % for Fe and Si, respectively. This is consistent with the narrowing of the electric field gradient (EFG) distribution and the appearance of nonzero occurrence frequency at null EFG after thermal annealing at 773 K. The higher yield $\chi_m(\mathrm{Fe})$ associated with backscattering from iron may originate from the poorer quality of the γ-FeSi$_2$ crystallites compared to the Si matrix. If this is the case, $\chi_m^{av}(\mathrm{Si})\approx 0.14$ would be the weighted average of the minimum yield from Si in the matrix, $\chi_m^{Si}(\mathrm{Si})$, and that from Si in γ-FeSi$_2$, $\chi_m^{\gamma}(\mathrm{Si})$. Assuming that $\chi_m^{\gamma}(\mathrm{Si})\approx\chi_m(\mathrm{Fe})\approx 0.60$, the experimental value $\chi_m^{av}(\mathrm{Si})=0.14$ is reproduced for $\chi_m^{Si}(\mathrm{Si})=0.09$, a reasonable value for IBIEC crystallized silicon.

The poor quality of the γ-FeSi$_2$ crystallites could be caused by the existence of a large number of vacancies and/or antisite defects. A few percent of these defects would give rise to a multiplicity of different atomic configurations. This in turn would lead to a broad distri-

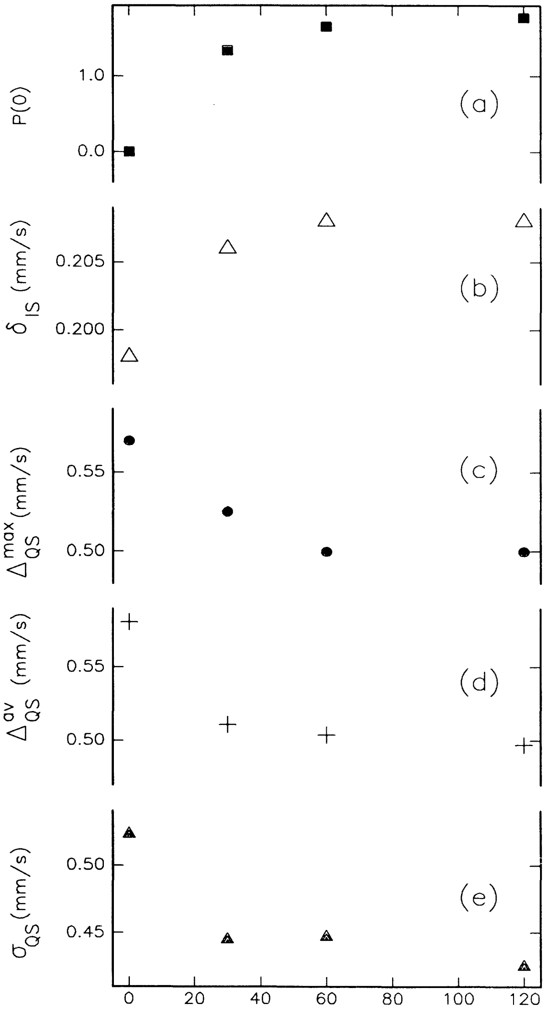

FIG. 3. Evolution with annealing time of the parameters associated with the hyperfine interaction at the ^{57}Fe site in γ-FeSi$_2$ (a) relative frequency occurrence of $\Delta_{QS}=0.0$ mm/s, (b) isomer shift, (c) the Δ_{QS} at the maximum occurrence frequency, (d) Δ_{QS} average, and (e) the full width at half maximum of the distribution. Isomer shifts are referred to as α-Fe.

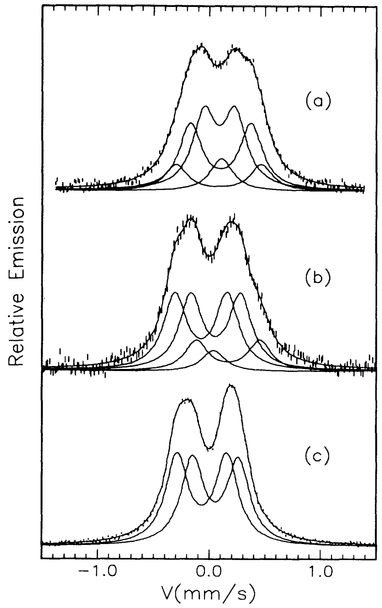

FIG. 4. RT CEMS spectra from samples annealed at different temperatures for 30 min. (a) 973 K, notice that the spectrum asymmetry becomes more pronounced indicating the beginning of the transformation of γ-FeSi$_2$ phases. (b) 1073 K; fraction of precipitates has transformed into β-FeSi$_2$ (two dominant doublets equally populated). (c) 1173 K; precipitates have been completely transformed into β-FeSi$_2$

bution of electric field gradients which was, in fact, observed.

In this sense the presence of the pseudomorphic CsCl-derived defect structure with statistical Fe-site occupation would also lead to an EFG distribution. However, this possibility can be rejected, because electron diffraction can easily distinguish the fluorite-type from the CsCl-type structures.[3]

Other potential sources of EFG and dechanneling are the Si/γ-FeSi$_2$ interfaces, where the dechanneling potential experiences a sudden change and the cubic symmetry around the Fe probes is lost. However, if there is no bulk disorder (inside the γ-FeSi$_2$ precipitates) the interface contribution to the EFG would most probably give rather discrete EFG values instead of the observed smooth distribution. For CoSi$_2$/Si(100) and NiSi$_2$/Si(100) interfaces (both silicides have a fluorite-type structure) different atomic structure models have been considered. Chernes, Hetherington, and Hymphreys[16] proposed two different models. In one of them the tetrahedral coordination of the Si atoms is preserved everywhere, while interfacial metal atoms are sixfold coordinated. In the second model the interfacial metal atoms are sixfold coordinated, while interfacial Si atoms are eightfold coordinated. Loretto, Gibson, and Yalisove[17] proposed that the interface is reconstructed in a 2×1 periodic array of Si dimers. Bulle-Lieuwma, de Jong, and Vandenhoudt[18] have found evidence of differences in composition rather than atomic displacements. Irrespective of the interface's defect structure, it is clear that Fe local environments are different and their eightfold coordination is not preserved, then δ_{IS} values must change from site to site.

It must be noticed that the isomer shift of ^{57}Fe in the γ-FeSi$_2$ phase is narrowly distributed. Since this quantity depends essentially on the number and the type of near neighbors, its uniformity indicates that the Si coordination number of the ^{57}Fe probes does not vary from site to site. This fact allows us to reject antisite defects as a source of EFG. Consistent with this, the existence of Si vacancies, which are all near neighbors to Fe atoms, should also be rejected as well as the different coordination of probes at interfaces.

The best defect candidates to explain our results are misplacement of Fe atoms in the γ-FeSi$_2$ lattice. In the fluorite-type structure the cubes formed by eight Si atoms are alternately filled with one Fe atom or otherwise empty. If a few percent of the Fe atoms are not at the expected places but randomly shifted to nearby empty cubes, a distribution of EFG would appear while the electron diffraction patterns would still correspond to γ-FeSi$_2$. For instance, if 10% of the Fe atoms were misplaced, about 60% of the ^{57}Fe probes would have at least one Fe neighbor at half a lattice parameter. For such a situation almost each probe in the sample will have a variable number of misplaced Fe atoms at higher-order neighbor locations.

Finally, we will comment briefly on the value of the γ-FeSi$_2$ isomer shift. This quantity has a relatively large positive value in conducting iron silicides [δ_{IS}(FeSi) $=0.27$ mm/s, δ_{IS}(α-FeSi$_2$)$=0.28$ mm/s] (Refs. 9 and 10) and a lower positive value in the semiconducting β-FeSi$_2$ ($\delta_{IS}^{av}=0.07$ mm/s).[9,10] A similar difference has been observed for the semiconducting to conducting transformation in amorphous Si$_{1-x}$Fe$_x$ ($0.2\leq x\leq0.5$).[19] The origin of a lower isomer shift value in the semiconducting phase is probably due to a stronger covalent character of the Fe-Si bonds, which increases the *s*-type character of the iron valence electrons via *d-sp* hybridization. The isomer shift of γ-FeSi$_2$ ($\delta_{IS}=0.206$ mm/s is therefore consistent with its reported conducting properties.[6]

Similar results have been reported for bulk CoSi$_2$, for a buried layer of CoSi$_2$ in Si produced by mesotaxy and for a CoSi$_2$ epitaxial surface layer prepared by MBE on Si.[20,21] For CoSi$_2$ buried layers in Si(111), the area of the doublet at 150 K is around 20–30% of the spectrum, while when the Si surface is (100), only a small contribution of the doublet was detected.[21] In all cases the spectra were analyzed with a single line plus a doublet. The origin of the quadrupole interaction was assigned to the presence of structural vacancies or defects with preferential orientation, or the occurrence of locally off-stoichiometry in a random way. But the interpretation of these anomalous MS spectra is not straightforward. It will be interesting to investigate if the EFG source is the same in both CoSi$_2$ and γ-FeSi$_2$ systems.

In summary, we have determined the hyperfine interactions associated with fluorite-type iron silicide. A broad distribution of EFG has been observed, which is unexpected in view of the cubic structure of γ-FeSi$_2$. The simultaneous consideration of TEM, ion channeling, and

Mössbauer results suggests that the EFG is originated from disorder in the iron sublattice. It is proposed that a fraction of Fe atoms do not occupy the expected Si cubes but are shifted to nearby empty ones.

The measured isomer shift is consistent with the metallic properties of γ-FeSi$_2$. Concerning the possible magnetic ordering of γ-FeSi$_2$, MS experiments below 17 K must be performed in order to confirm the Hall resistivity results,[7] since at 17 K the MS spectrum did not show magnetic splitting nor broadening.

ACKNOWLEDGMENTS

This work was partially supported by Programa TENAES of Consejo Nacional de Investigaciones Científicas y Técnicas (CONICET) and Fundación Antorchas, Argentina. The authors are indebted to M. O. Katisov for the iron implantation and to Dr. R. C. Mercader and Dr. M. S. Moreno for technical assistance with low-temperature MS measurements.

[1] H. von Kanel, Mater. Sci. Rep. **8**, 193 (1992).

[2] S. Mantl, Mater. Sci. Rep. **8**, 1 (1992).

[3] H. Sirringhaus, N. Onda, E. Müller-Gubler, P. Müller, R. S. Stalder, and H. von Kanel, Phys. Rev. B **47**, 10 567 (1993).

[4] N. Onda, J. Henz, E. Müller, K. A. Mader, and H. von Kanel, Appl. Surf. Sci. **56-58**, 421 (1992).

[5] J. Chevrier, V. Le Thanh, S. Nitzche, and J. Derrien, Appl. Surf. Sci. **56-58**, 438 (1992); M. G. Grimaldi, P. Baeri, C. Spinella, and S. Lagomarsino, Appl. Phys. Lett. **60**, 1132 (1992).

[6] N. E. Christensen, Phys. Rev. B **42**, 7148 (1990).

[7] N. Onda, J. Henz, K. A. Müller, K. A. Mader, and H. von Kanel (unpublished).

[8] J. Desimoni, H. Bernas, M. Behar, X. W. Lin, J. Washburn, and Z. Liliental-Weber, Appl. Phys. Lett. **62**, 306 (1993); X. W. Lin, M. Behar, J. Desimoni, H. Bernas, Z. Liliental-Weber, and J. Washburn, Appl. Phys. Lett. **63**, 105 (1993); X. W. Lin, J. Desimoni, H. Bernas, Z. Liliental-Weber, and J. Washburn, *Phase Transformations in Thin Films—Thermodynamics and Kinetics*, edited by M. Atzmon, A. L. Greer, J. M. E. Harper, and M. R. Libera, MRS Symposia Proceedings No. 311 (Materials Research Society, Pittsburgh, 1993), p. 293.

[9] K. Vojtyzechovsky and T. Zémcik, Czech. J. Phys. B **24**, 171 (1974).

[10] R. Wandji, Phys. Status Solidi B **45**, K123 (1971).

[11] S. Degroote, M. H. Langhlaar, T. Kobayashi, J. Dekoster, J. De Wachter, R. Moons, L. Niesen, and G. Langouche, *Phase Transformations in Thin Films—Thermodynamics and Kinetics* (Ref. 8), p. 133.

[12] H. Bernas, J. Chaumont, E. Cotterau, R. Meunir, A. Traverse, C. Clerc, O. Katisov, F. Lalu, D. Le Duc, G. Moroy, and M. Salomé, Nucl. Instrum. Methods B **62**, 416 (1992).

[13] R. E. Vandenberghe (private communication).

[14] P. B. Hirsch, A. Howie, R. B. Nicholson, D. W. Pashly, and M. J. Whelan, in *Electronics Microscopy of Thin Crystals,* 2nd ed. (Krieger, Malabar, FL, 1977).

[15] G. Langouche, Hyperfine Interact. **72**, 217 (1992).

[16] D. Cherns, C. J. D. Hetherington, and C. J. Hymphreys, Philos. Mag. A **49**, 161 (1984).

[17] D. Loretto, J. M. Gibson, and S. M. Yalisove, Phys. Rev. Lett. **63**, 298 (1989).

[18] C. W. T. Bulle-Lieuwma, A. F. de Jong, and D. E. W. Vandenhoudt, Philos. Mag. A **64**, 255 (1991).

[19] F. H. Sánchez, M. B. Fernández van Raap, and J. Desimoni, Phys. Rev. B **44**, 4290 (1991).

[20] W. G. Spanninga, P. J. M. Smulders, and L. Niesen, Nucl. Instrum. Methods B **63**, 138 (1992).

[21] G. Langouche, M. de Potter, I. Dézsi, M. F. Wu, and A. Vantomme, Nucl. Instrum. Methods B **37**, 438 (1989).

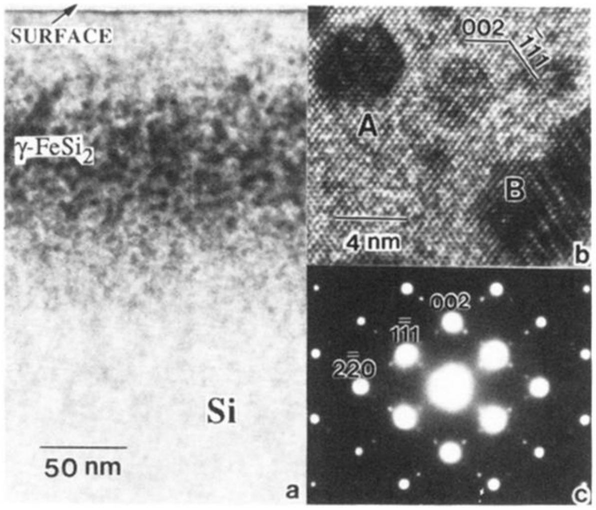

FIG. 1. TEM micrographs showing the presence of γ-FeSi$_2$ precipitates in an Fe-implanted Si sample first treated by IBIEC at 593 K and subsequently annealed at 773 K for 1 h. (a) Cross-sectional bright-field image showing the distribution of γ-FeSi$_2$ precipitates (dark region below the surface). (b) High-resolution image of *A*-type and *B*-type γ-FeSi$_2$ precipitates, viewed along Si[110]. (c) Selected-area diffraction spots correspond to reflections from the Si[110] zone axis, while the weak ones are due to reflections from *B*-type γ-FeSi$_2$ precipitates, combined with double diffraction effects.